



Research Repository UCD

Title	Phase jitter dynamics of first-order digital phase-locked loops with frequency-modulated input
Authors(s)	Tertinek, Stefan, Teplinsky, Alexey, Feely, Orla
Publication date	2008-05-18
Publication information	Tertinek, Stefan, Alexey Teplinsky, and Orla Feely. "Phase Jitter Dynamics of First-Order Digital Phase-Locked Loops with Frequency-Modulated Input." IEEE, 2008.
Conference details	IEEE International Symposium on Circuits and Systems (ISCAS), Seattle, USA, 18-21 May 2008
Publisher	IEEE
Item record/more information	http://hdl.handle.net/10197/3593
Publisher's statement	Personal use of this material is permitted. Permission from IEEE must be obtained for all other uses, in any current or future media, including reprinting/republishing this material for advertising or promotional purposes, creating new collective works, for resale or redistribution to servers or lists, or reuse of any copyrighted component of this work in other works.
Publisher's version (DOI)	10.1109/ISCAS.2008.4541725

Downloaded 2024-03-28T04:02:09Z

The UCD community has made this article openly available. Please share how this access benefits you. Your story matters! (@ucd_oa)



© Some rights reserved. For more information

Phase Jitter Dynamics of First-Order Digital Phase-Locked Loops with Frequency-Modulated Input

Stefan Tertinek*, Alexey Teplinsky†, and Orla Feely*

*School of Electrical, Electronic and Mechanical Engineering, University College Dublin, Belfield, Dublin 4, Ireland
Email: stertinek@ee.ucd.ie, orla.feely@ucd.ie

†Institute of Mathematics, National Academy of Sciences of Ukraine, 3 Tereshchenkivska St, Kiev 01601, Ukraine
Email: teplinsky@imath.kiev.ua

Abstract—Inherent to digital phase-locked loops is frequency quantization in the number-controlled oscillator which prevents the loop from locking exactly onto its reference signal and introduces unwanted phase jitter. This paper investigates the effect of frequency quantization in a first-order loop with a frequency-modulated input signal. Using tools of nonlinear dynamics, we show that, depending on the modulation amplitude, trajectories in the phase space eventually fall into either an invariant region or a trapping region, the boundaries of which give useful bounds on the steady-state phase jitter excursion. We also derive a sufficient condition for the maximum modulation amplitude to prevent loop cycle slipping.

I. INTRODUCTION

Phase-locked loops (PLLs) are used in many electronic systems, particularly in frequency synthesis and clock recovery circuits [1]. In essence, a PLL synchronizes the phase of a controlled oscillator to the phase of a reference signal by operating the oscillator together with a phase detector and a loop filter in a closed loop. Once the loop is locked, i.e., the phase difference between the two signals is zero or constant, the feedback forces the oscillator to track phase variations of the reference signal, allowing the system to demodulate frequency-modulated (FM) signals. Digital phase-locked loops (DPLLs) typically contain a number-controlled oscillator (NCO) whose output signal can have only a finite number of different frequencies. This frequency quantization results in phase locking with jitter: unwanted oscillatory steady-state motion of the phase error about its locked state. For a sinusoidal input signal, many results on the effect of frequency quantization that were obtained by Gardner using extensive simulations [2] were rigorously verified using the theory of nonlinear dynamics [3],[4]. For an FM input signal, previous works were mainly concerned with the global nonlinear dynamics of the unquantized loop, and only preliminary results were obtained in the case of frequency quantization [5]. Recently, a nonlinear dynamics approach has also enabled a rigorous analysis of bang-bang PLLs [6].

To gain further insight into the effect of frequency quantization in a DPLL, this paper shall investigate the steady-state phase jitter dynamics of a first-order loop with an FM input signal. Based on the results in [7], we show that for a sufficiently small modulation amplitude, the loop behavior can be described by the map of a first-order sigma-delta modulator with a sampled periodic input signal, and trajectories eventually fall into an invariant belt (a belt-shaped region in the phase space). For a large amplitude, there exists a trapping belt which, upon entering, trajectories cannot leave. In either case, the boundaries of the belts give useful bounds on the steady-state phase jitter excursion and allow us to determine a sufficient condition for the maximum modulation amplitude to prevent loop cycle slipping.

II. FIRST-ORDER DPLL MODEL

A phase domain model of the first-order DPLL under investigation is shown in Fig. 1 [2],[4]. The phase detector compares the phase of

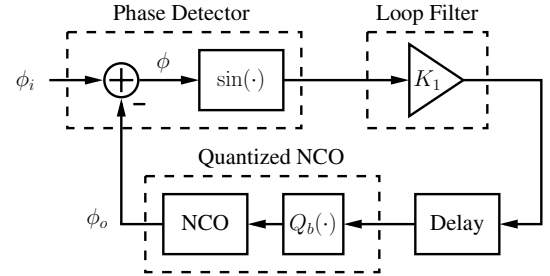


Fig. 1. Phase domain model of a first-order digital phase-locked loop.

the input (or reference) signal, ϕ_i , with the phase of the NCO output signal, ϕ_o , and produces an output equal to the sine of the phase error $\phi = \phi_i - \phi_o$. After scaling by the gain coefficient K_1 , the output of the loop filter drives the quantized NCO so as to minimize the phase error ϕ . For an FM input signal, the phase error can be modeled by the nonlinear first-order difference equation [5]

$$\phi_{n+1} = \phi_n + 2\pi\nu + A \cos(\omega(n+1) + \theta_0) - 2\pi Q_b(K_1 \sin \phi_n) \mod 2\pi \quad (1)$$

where we assume that the carrier frequency ν is positive and that $2^b\nu$ is not an integer. The sinusoidal modulation signal, in the following referred to as the forcing term, has amplitude A , initial phase θ_0 and frequency ω , where $\omega/(2\pi)$ is assumed to be irrational. The b -bit quantizer, denoted by its input-output characteristic $Q_b(\cdot)$, is responsible for the NCO frequency quantization. The most common are uniform quantizers with a midtread or midrise characteristic [8]. To simplify the discussion, we assume a midrise quantizer of the form $Q_b(x) = \lfloor 2^b x \rfloor / 2^b$ which has a riser at zero [2]; the symbol $\lfloor \cdot \rfloor$ refers to the floor function which gives the largest integer less than or equal to its argument.

The difference equation in (1) is nonautonomous due to the explicit presence of the discrete-time variable n . By introducing the argument of the cosine as a new variable, we can convert (1) into the nonlinear autonomous system of two difference equations

$$\theta_{n+1} = \theta_n + \omega \mod 2\pi \quad (2)$$

$$\phi_{n+1} = \Phi(\theta_{n+1}, \phi_n) \mod 2\pi \quad (3)$$

where

$$\Phi(\theta, \phi) = \phi + 2\pi\nu + A \cos \theta - \frac{2\pi}{2^b} \lfloor 2^b K_1 \sin \phi \rfloor. \quad (4)$$

These equations define a map of the torus $\mathbf{S}_{2\pi} \times \mathbf{S}_{2\pi}$ onto itself, where $\mathbf{S}_{2\pi} = \mathbf{R} \mod 2\pi$ denotes the circle of length 2π . The aim in the following sections is to investigate the limit behavior of trajectories $\{(\theta_n, \phi_n)\}_{n=0}^\infty$ of this map in the 2D phase space.

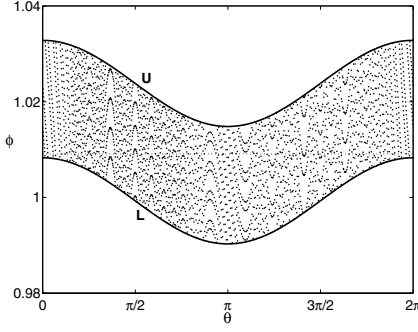


Fig. 2. Invariant belt B with continuous boundaries U and L for small forcing $0 < A < A_0$. Parameters: $A = 0.009$, $\omega = 0.005$, $b = 8$, $\nu = 0.1$, $K_1 = 0.12$.

III. INVARIANT BELT FOR SMALL FORCING

A. Without Forcing ($A = 0$)

In [3] a first-order DPLL with a sinusoidal input signal was studied (the map (3) – (4) with $A = 0$). It was found that under certain conditions on ν and K_1 , a trajectory in the phase space eventually falls into an invariant trapping region in which its steady-state behavior obeys a circle rotation. This region consists of two segments of the graph, corresponding to two adjacent quantizer values, which are separated by a discontinuity at the phase value

$$\phi_d = \sin^{-1} \left(\frac{\lfloor 2^b \nu \rfloor + 1}{2^b K_1} \right). \quad (5)$$

Below this discontinuity, the trajectory increases by $(2\pi/2^b) \text{Frac}[2^b \nu]$ with each iteration, whereas it decreases by $(2\pi/2^b)(1 - \text{Frac}[2^b \nu])$ above. More generally, this steady-state behavior can be written as the one-parameter family of interval shifts

$$\phi_{n+1} = \begin{cases} \phi_n - d_1, & \phi_d \leq \phi_n < \phi_{\max} \\ \phi_n + d_2, & \phi_{\min} \leq \phi_n < \phi_d \end{cases} \quad (6)$$

where $d_1 = (2\pi/2^b)(1 - \text{Frac}[2^b \nu])$, $d_2 = (2\pi/2^b) \text{Frac}[2^b \nu]$, and ϕ_{\min} and ϕ_{\max} are the endpoints of the invariant trapping region.

B. With Small Forcing

If we now consider the map (2) – (4) with sufficiently small forcing A , the parameters d_1 and d_2 in (6) become dependent on θ , i.e., $d_1(\theta) = (2\pi/2^b)(1 - \text{Frac}[2^b \nu]) - A \cos \theta$ and $d_2(\theta) = (2\pi/2^b) \text{Frac}[2^b \nu] + A \cos \theta$. We can therefore write (6) as the one-parameter family of driven interval shifts

$$\phi_{n+1} = \phi_n + f(\theta_{n+1}) - g \text{sgn}(\phi_n - \phi_d) \quad (7)$$

where the driving (or forcing) term

$$f(\theta) = \frac{1}{2}(d_2(\theta) - d_1(\theta)) = \frac{\pi}{2^b}(2 \text{Frac}[2^b \nu] - 1) + A \cos \theta \quad (8)$$

and the signum function, defined as $\text{sgn } x = 1$ for $x \geq 0$, and $\text{sgn } x = -1$ for $x < 0$, is scaled by

$$g = \frac{1}{2}(d_1(\theta) + d_2(\theta)) = \frac{\pi}{2^b}. \quad (9)$$

The difference equation (7), which describes a first-order sigma-delta modulator with a sampled periodic input signal, was rigorously studied in [7]. It follows from that work that under the condition $|f| < g$, all trajectories eventually fall into the invariant belt

$$B = \{(\theta, \phi) | L(\theta) \leq \phi < U(\theta), \theta \in \mathbf{S}_{2\pi}\} \quad (10)$$

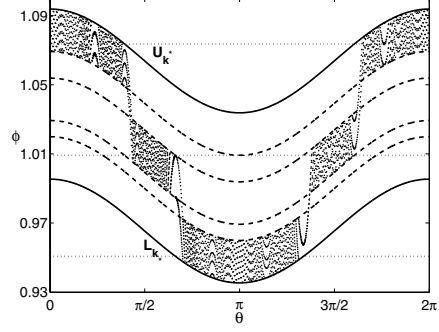


Fig. 3. Trapping belt T with continuous boundaries U_{k^*} and L_{k^*} for large forcing $A_0 \leq A \leq A_1$. Parameters as in Fig. 2, but with $A = 0.03$.

with continuous boundaries

$$U : \quad \phi = \phi_d + \frac{2\pi}{2^b} \text{Frac}[2^b \nu] + A \cos \theta \quad (11)$$

$$L : \quad \phi = \phi_d + \frac{2\pi}{2^b} (\text{Frac}[2^b \nu] - 1) + A \cos \theta \quad (12)$$

and constant vertical thickness $2\pi/2^b$. Using (8) and (9), the condition $|f| < g$ implies

$$A < A_0 = \frac{2\pi}{2^b} \min\{\text{Frac}[2^b \nu], 1 - \text{Frac}[2^b \nu]\}. \quad (13)$$

In summary, for A less than A_0 , the belt B in (10) is invariant under the map (2) – (4), is bounded by the continuous curves U and L given by (11) and (12), respectively, and has constant vertical thickness $2\pi/2^b$. Figure 2 shows 3000 points of a trajectory with the first 100 points discarded. For the given parameters, $A < A_0 \approx 0.009817$ and the trajectory eventually falls into the invariant belt B bounded by the solid curves. The dotted line within the belt corresponds to the discontinuity at the phase value in (5). It was pointed out in [7] that U and L are the images of this discontinuity line under the map from below and above this line. In the following, we will show how we can use this fact to construct a trapping belt in the case of large forcing A .

IV. TRAPPING BELT FOR LARGE FORCING

In this section, we will consider the case when A exceeds the bound in (13) and construct a trapping belt which, upon entering, trajectories cannot leave. An example of this belt is shown in Fig. 3, which plots 3000 points of a trajectory with the first 100 points discarded. Since $A \geq A_0$ for the given parameters, the trajectory cannot fit into the belt (10) but is trapped in a wider belt (the region between the solid curves in the figure).

To begin the construction of the trapping belt, let us write (2) – (4) in a more convenient form. Assume that $2^b K_1$ is not an integer, and denote $k_{\max} = \lfloor 2^b K_1 \rfloor$. It can be seen from (4) that the discontinuities of Φ , which are the quantizer threshold values, do not depend on θ ; for $-k_{\max} \leq k \leq k_{\max}$, $k \in \mathbf{Z}$, they are given by

$$\sigma_k^+ = \sin^{-1} \left(\frac{k}{2^b K_1} \right) \quad (14)$$

for those $\phi \in \mathbf{S}_{2\pi}$ where $\sin \phi$ has a positive slope (the ascending branch), and

$$\sigma_k^- = \pi - \sigma_k^+ \quad (15)$$

for those $\phi \in \mathbf{S}_{2\pi}$ where $\sin \phi$ has a negative slope (the descending branch). These discontinuities divide the circle in ϕ into the $4k_{\max} + 2$

intervals

$$\Delta_k = \begin{cases} [\sigma_{k_{\max}}^+, \sigma_{k_{\max}}^-], & k = k_{\max} \\ [\sigma_k^+, \sigma_{k+1}^+) \cup (\sigma_{k+1}^-, \sigma_k^-], & -k_{\max} \leq k \leq k_{\max} - 1 \\ (\sigma_{-k_{\max}}^-, \sigma_{-k_{\max}}^+), & k = -k_{\max} - 1 \end{cases} \quad (16)$$

where each corresponds to one of the $2k_{\max} + 2$ quantizer output values. Hence, for $\phi \in \Delta_k$, $-k_{\max} - 1 \leq k \leq k_{\max}$, we can write (2) – (4) as

$$F_k(\theta, \phi) = (\theta + \omega, \phi + c_k + A \cos(\theta + \omega)) \mod 2\pi \quad (17)$$

where $c_k = 2\pi\nu - (2\pi/2^b)k$. The 2D phase space is therefore divided into $4k_{\max} + 2$ strips, where each two adjacent ones are separated by the discontinuity line $D_k^+ = \mathbf{S}_{2\pi} \times \{\sigma_k^+\}$ on the ascending sine branch and by the discontinuity line $D_k^- = \mathbf{S}_{2\pi} \times \{\sigma_k^-\}$ on the descending sine branch (both series of lines are shown dotted in Fig. 3). The map in its form (17) can now be used to construct the trapping belt. In the previous section, we have seen that for $A < A_0$, the upper and lower boundaries of the invariant belt B are the images of the discontinuity line $\mathbf{S}_{2\pi} \times \{\phi_d\}$ under the map from below and above this line. Consider now the images of the k th discontinuity line D_k^+ under the map (17) from below and above this line; i.e.,

$$U_k : \quad \phi = \sigma_k^+ + c_{k-1} + A \cos \theta \quad (18)$$

$$L_k : \quad \phi = \sigma_k^+ + c_k + A \cos \theta \quad (19)$$

where $U_k = F_{k-1}(D_k^+)$ and $L_k = F_k(D_k^+)$ (both series of curves are shown dashed in Fig. 3). We define the trapping belt as the bounded set

$$T = \{(\theta, \phi) | L_{k_*}(\theta) \leq \phi < U_{k^*}(\theta), \theta \in \mathbf{S}_{2\pi}\} \quad (20)$$

where the upper boundary U_{k^*} and the lower boundary L_{k_*} are the curves in (18) and (19), respectively, with k replaced by the integers k^* and k_* (the solid curves in Fig. 3). To determine these two integers, we will use the results from [7]. Let us consider the vertical segment $[L_k(\theta), U_k(\theta))$ for some $\theta \in \mathbf{S}_{2\pi}$. To find k^* corresponding to the upper boundary of T , we take $\theta = 0$ to get the maximum of U_k . Now, if $\sigma_k^+ \in (L_k(0), U_k(0))$, i.e., σ_k^+ falls into the interior of this segment, then this point splits the segment into two half-open segments, where the upper part $[\sigma_k^+, U_k(0))$ is shifted by the map F_k , and the lower part $[L_k(0), \sigma_k^+)$ is shifted by the map F_{k-1} , such that their images exchange their places without an overlap or a gap. This implies in particular that if U_k was the upper boundary of the trapping belt T , then a trajectory approaching it from below could not jump above it. Therefore, we must find k such that $U_k(0) \geq \sigma_k^+$ and $L_k(0) < \sigma_k^+$. Using (18) and (19), this gives

$$2^b\nu + \frac{2^b A}{2\pi} < k \leq 2^b\nu + \frac{2^b A}{2\pi} + 1. \quad (21)$$

Since k must be an integer, we obtain

$$k^* = \left\lfloor 2^b\nu + \frac{2^b A}{2\pi} \right\rfloor + 1. \quad (22)$$

To find k_* corresponding to the lower boundary of T , we take $\theta = \pi$ to get the minimum of L_k . By a similar argument, we must find k such that $U_k(\pi) \geq \sigma_k^+$ and $L_k(\pi) < \sigma_k^+$. Using (18) and (19), we obtain the required integer

$$k_* = \left\lfloor 2^b\nu - \frac{2^b A}{2\pi} \right\rfloor + 1. \quad (23)$$

Since k^* and k_* depend on A , and thus also the vertical thickness of T , we will now determine the minimum and maximum A such that the trapping belt is given by (20). First, for A less than a minimum

value A_0 , the trapping belt T will coincide with the invariant belt B in (10). Since A_0 is obtained by setting $k^* = k_*$, removing the integer part of $2^b\nu$ in (22) and (23) gives

$$\left\lfloor \text{Frac}[2^b\nu] + \frac{2^b A}{2\pi} \right\rfloor = \left\lfloor \text{Frac}[2^b\nu] - \frac{2^b A}{2\pi} \right\rfloor. \quad (24)$$

This equation is satisfied if $\text{Frac}[2^b\nu] + 2^b A/(2\pi) < 1$ and $\text{Frac}[2^b\nu] - 2^b A/(2\pi) > 0$, from which A_0 in (13) follows. Note that for $A < A_0$, we have $k^* = k_* = \lfloor 2^b\nu \rfloor + 1$, and inserting into (14) gives the corresponding discontinuity in (5). Second, for A larger than a maximum value A_1 , the trajectory will leave the maximum upper belt boundary $U_{k_{\max}}$ and cycle slipping may occur, which will be discussed in Sec. VI. To find A_1 , let us take a closer look at the strip $\mathbf{S}_{2\pi} \times \Delta_{k_{\max}}$. It follows from (14) – (16) that its vertical thickness $\Delta_{k_{\max}}$ can be made arbitrarily narrow by a proper choice of K_1 . Since the upper belt boundary $U_{k_{\max}}$ extends into this strip, we must ensure that it does not collide with the repelling discontinuity line $D_{k_{\max}}^-$, for a particular choice of K_1 . For simplicity, we set $U_{k_{\max}}(0) = \sigma_{k_{\max}}^+$ to prevent $U_{k_{\max}}$ from extending into this strip. Since $U_k(0) \geq \sigma_k^+$ was a condition to derive (21), substituting $k_{\max} = \lfloor 2^b K_1 \rfloor$ into that equation gives

$$A_1 = \frac{2\pi}{2^b} (\lfloor 2^b K_1 \rfloor - 1) - 2\pi\nu. \quad (25)$$

Note further that since we assume $\nu > 0$, we do not need to consider the case when the trajectory will leave the minimum lower belt boundary $L_{-k_{\max}}$.

V. INVARIANT CURVES AND DYNAMICS WITHIN THE BELTS

The sinusoidal forcing term allows us to derive the invariant curves of the map (17) in closed form and to determine the dynamics within the belts. The invariant curves for the case $c_k = 0$ were derived in [7]. Using that result and the fact that c_k is multiplied by n after n iterations, we get

$$\phi_n = \phi_0 + c_k n + A' \left[\sin\left(\theta_0 + \omega n + \frac{\omega}{2}\right) - \sin\left(\theta_0 + \frac{\omega}{2}\right) \right] \quad (26)$$

where $A' = A/(2 \sin(\omega/2))$. With $\theta_n = \theta_0 + \omega n$ and $c_k n \equiv c_k(\theta_n - \theta_0) / \omega$, we can write

$$\phi_n = \frac{c_k}{\omega} \theta_n + A' \sin\left(\theta_n + \frac{\omega}{2}\right) + C(\theta_0, \phi_0) \quad (27)$$

where $C(\theta_0, \phi_0) = \phi_0 - c_k \theta_0 / \omega - A' \sin(\theta_0 + \omega/2)$, and thus get the invariant curves

$$I_k : \quad \phi = \frac{c_k}{\omega} \theta + A' \sin\left(\theta + \frac{\omega}{2}\right) + C(\theta_0, \phi_0) \quad (28)$$

inside the strip $\mathbf{S}_{2\pi} \times \Delta_k$, $-k_{\max} - 1 \leq k \leq k_{\max}$.

To gain insight into the dynamics within the belts, recall that the unforced system has a periodic point of period N if $2^b N \nu$ is an integer [3]. Thus, for rational ν , a trajectory starting at the point (θ_0, ϕ_0) will reside on the set

$$S(\theta_0, \phi_0) = \bigcup_{m \in \mathbf{Z}} S_m(\theta_0, \phi_0) \quad (29)$$

that consists of the sinusoids

$$S_m(\theta_0, \phi_0) : \quad \phi = A' \sin\left(\theta + \frac{\omega}{2}\right) + \phi_0 - A' \sin\left(\theta_0 + \frac{\omega}{2}\right) + \frac{2\pi}{2^b} \frac{m}{N}. \quad (30)$$

At each iteration, the trajectory will jump between one of the N sets

$$R_j(\theta_0, \phi_0) = \bigcup_{\substack{m=iN+j \\ i \in \mathbf{Z}}} S_m(\theta_0, \phi_0) \quad (31)$$

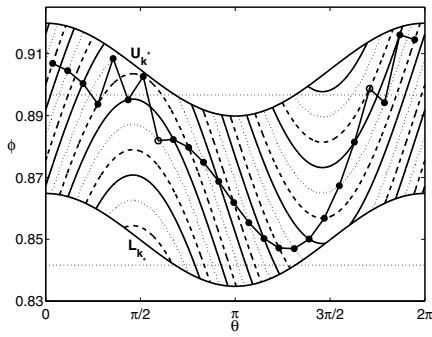


Fig. 4. For rational ν , a trajectory within the trapping belt resides on the three sets R_0 (solid), R_1 (dashed) and R_2 (dotted), as shown for one full rotation in θ . Parameters: $A = 0.015$, $\omega = 0.25$, $b = 8$, $\nu = 1/12$, $K_1 = 0.11$.

for $0 \leq j \leq N-1$. Figure 4 shows an example of a trapping belt and a trajectory for one full rotation in θ . For the given parameters, $2^b N \nu$ is an integer for $N = 3$, and the trajectory will jump between the sets R_0 , R_1 and R_2 . Since $\omega/(2\pi)$ is irrational, the trajectory densely fills parts of these three sets within the belt. For irrational ν , however, the unforced system cannot have a periodic point of period N since $2^b N \nu$ cannot be an integer. Thus, the trajectory will not reside on a finite set of sinusoids but densely fill a subset of the whole belt. Notice also in the figure that the points of the trajectory between the two empty circles lie on the invariant curve I_{k*} in (28) since the trajectory stays within the strip $S_{2\pi} \times \Delta_{k*}$.

VI. ACQUISITION BEHAVIOR AND CYCLE SLIPPING

So far, we have investigated the limit behavior of trajectories and have thereby obtained useful bounds on the steady-state phase jitter excursion of the locked loop. In the design of a DPLL, however, phase acquisition must also be taken into account. To clarify this process, we will remove the mod 2π term in (3) such that the phase space becomes the upright standing cylinder shell $S_{2\pi} \times \mathbf{R}$. The picture of a trajectory in the phase space will then repeat every 2π , depending on its origin on the cylinder shell. This relation is illustrated in Fig. 5, which shows 1000 points of two trajectories (the first 100 points were again removed) whose origins in the phase space differ by 2π in ϕ .

For the purpose of illustration, we begin by investigating the map (17) for $A = 0$ (unmodulated case). Consider a trajectory starting on or just below the discontinuity line $D_{k\nu+1}^-$ (shown in Fig. 5 by the dashed lines), where $k_\nu = \lfloor 2^b \nu \rfloor$. It follows from (17) that the trajectory will decrease with each iteration since $c_{k\nu+1} = (2\pi/2^b)(\text{Frac}[2^b \nu] - 1) < 0$. Conversely, a trajectory starting just above $D_{k\nu+1}^-$ will increase with each iteration since $c_{k\nu} = (2\pi/2^b)\text{Frac}[2^b \nu] > 0$. Hence, $D_{k\nu+1}^-$ is a repelling discontinuity line which corresponds to the unstable fixed point $\phi = \pi - \sin^{-1}(\nu/K_1)$ in a DPLL without frequency quantization.

Consider now the map for $0 < A < A_0$ and a trajectory starting again on or just below the discontinuity line $D_{k\nu+1}^-$. Since the forcing is too small to carry the trajectory above $D_{k\nu+1}^-$, the trajectory will move downwards on the cylinder shell and eventually fall into the invariant belt. Similarly, a trajectory starting just above $D_{k\nu+1}^-$ will move upwards and eventually fall into the invariant belt a distance 2π above the other. If we now increase the forcing such that $A_0 \leq A \leq A_1$, then, for a range of $\theta \in S_{2\pi}$, a trajectory starting within a certain distance below (above) $D_{k\nu+1}^-$ will move upwards (downwards) and finally end up in the corresponding trapping belt. The result is a repelling contour (depicted in Fig. 5 by the solid

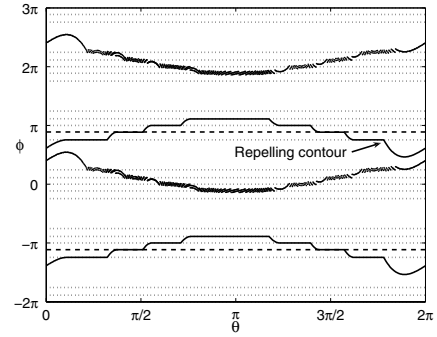


Fig. 5. The trajectory does not fit in a trapping belt for $A > A_1$. Parameters: $A = 0.35$, $\omega = 0.01$, $b = 5$, $\nu = 0.01$, $K_1 = 0.09$.

curves), which could be thought of as bending the discontinuity line $D_{k\nu+1}^-$ along the θ axis. The detailed construction of this contour is given in [9].

In the above cases, a trajectory starting at a certain point in the phase space and approaching a belt will not cover a distance of more than 2π in the ϕ direction since the belts repeat every 2π ; thus, there is no cycle slipping in the acquisition process [1]. A different behavior may be observed if $A > A_1$, as depicted in Fig. 5. For the given parameters, the trajectory does not fit in a trapping belt but extends above the curve $U_{k_{\max}}$. By increasing A further, trajectories will eventually jump above the repelling contour at some point and move upwards on the cylinder shell, thus slipping one cycle (or covering a distance of more than 2π). Choosing $A \leq A_1$ in (25) gives a sufficient condition for the maximum amplitude such that loop cycle slipping is avoided.

VII. CONCLUSIONS

Continuing previous works for a sinusoidal input signal, this paper has investigated the effect of frequency quantization in a first-order DPLL with an FM input signal. We have seen how a nonlinear analysis allows us to describe the behavior of trajectories in the phase space, to deduce bounds on the steady-state phase jitter excursion, and to derive a sufficient condition for the maximum modulation amplitude to prevent loop cycle slipping. The results can guide the designer in the implementation of these important systems.

REFERENCES

- [1] F. M. Gardner, *Phaselock Techniques*, 3rd ed. John Wiley & Sons, 2005.
- [2] —, “Frequency granularity in digital phaselock loops,” *IEEE Trans. Commun.*, vol. 44, no. 6, pp. 749–758, June 1996.
- [3] A. Rogers, D. Naughton, and O. Feely, “Nonlinear analysis of digital phase-locked loops,” in *Proc. ECCTD’97*, Budapest, September 1997, pp. 121–126.
- [4] A. Teplinsky, O. Feely, and A. Rogers, “Phase jitter dynamics of digital phase-locked loops,” *IEEE Trans. Circuits Syst. I*, vol. 46, no. 5, pp. 545–558, May 1999.
- [5] O. Feely, “Nonlinear dynamics of first-order DPLL with FM input,” in *Proc. ISCAS’00*, vol. 4, Geneva, May 2000, pp. 477–480.
- [6] A. Teplinsky, R. Flynn, and O. Feely, “Limit cycles in bang-bang phase-locked loops,” in *Proc. ISCAS’06*, vol. 3, Kos, May 2006, pp. 4074–4077.
- [7] A. Teplinsky, E. Condon, and O. Feely, “Driven interval shift dynamics in sigma-delta modulators and phase-locked loops,” *IEEE Trans. Circuits Syst. I*, vol. 52, no. 6, pp. 1224–1235, June 2005.
- [8] H. Roh and K. Cheun, “A modified midtread frequency quantization scheme for digital phase-locked loops,” *IEICE Trans. Commun.*, vol. E87-B, no. 3, pp. 752–755, March 2004.
- [9] S. Tertinek, A. Teplinsky, and O. Feely, “Frequency quantization in first-order digital phase-locked loops with frequency-modulated input,” in *Proc. Int. Workshop on Nonlinear Maps and their Applications, NOMA’07*, Toulouse, December 2007.